

Aqueous oxidation reaction enabled layer-by-layer corrosion of semiconductor nanoplates into single-crystalline 2D nanocrystals with single layer accuracy and ionic surface capping

Muwei Ji ^a, Meng Xu^a, Jun Zhang^b, Jiajia Liu^a, and Jiatao Zhang^{a,*}

a. Beijing Key Laboratory of Construction Tailorable Advanced Functional Materials and Green Applications, School of Materials Science and Engineering, Beijing Institute of Technology, Beijing, 100081, China

b. Institute of semiconductors, Chinese Academy of Sciences, Beijing, 100083, China

Corresponding Author

zhangjt@bit.edu.cn

Present Addresses

Beijing Institute of Technology, Beijing 100081, China. Tel.: +86 10 68918065; Fax: +86 10 68918065. E-mail: zhangjt@bit.edu.cn.

Experiment

Chemical and reagents: All of reagents are analytical grade and employed without further purification. Ethylene glycol (EG) and Sodium hydroxide (NaOH) are purchased from Tianjin Guangfu Fine Chemical Research Institute. Polyvinylpyrrolidone (PVP, K30, MW: 30000) and Bismuth Chloride (BiCl_3) are purchased from Sinopharm Chemical Reagent Co., Ltd., while potassium tellurite (K_2TeO_3) is purchased from Aladdin Chemical Co., Ltd..

Synthesis of Bi_2Te_3 nanoplate: Bi_2Te_3 nanoplates is prepared by following the Zhao's reports with some modified¹. In typically, PVP (K30, 4.44g) is dissolved in ethylene-glycol (EG, 40 mL) and then K_2TeO_3 (1.2 mmol), BiCl_3 (0.8 mmol) and NaOH (10 mmol) are placed under stirring in room temperature. After the chemicals dissolved, the resultant mixture is sealed in Teflon autoclave and heated to 180 °C, keeping at that temperature for 36 hours. The raw product is purified by washing with ethanol or methanol and centrifugation then re-dispersed in anhydrous methanol.

Oxidation of Bi_2Te_3 nanoplate: Bi_2Te_3 nanoplates (2 mL) is purified by washing with anhydrous methanol (2 mL) and centrifugation, and then re-dispersed in anhydrous methanol (4 mL). Then, ultrapure water (10 mL), NaOH aqueous solution (1 M, 0.1 mL) and H_2O_2 (30%) are added and stirred for 3 hours at room temperature. Then the raw products are purified by washing with anhydrous methanol and centrifugation. And the oxidation using other oxidized reagent, such as HNO_3 or $\text{Fe}(\text{NO}_3)_3$, is carried out in the Bi_2Te_3 methanol solution. In typically, into Bi_2Te_3 methanol solution, HNO_3 (3%) or $\text{Fe}(\text{NO}_3)_3$ (0.1 M, 1 mL) aqueous solution is added and the resultant mixture is purified by washing and centrifugation after stirring 3 hours.

Characterizations: The XRD pattern of samples are collected by using Bruker D8 multiply crystals X-ray diffractometer ($10^\circ/\text{min}$). Low resolution transmission electron microscope (LRTEM) images are obtained by HITACHI H-7650 electron microscopy operating at 80 kV. High resolution TEM, element mapping and energy dispersive X-ray spectroscopy (EDS) are perform on FEI Tecnai G2 F20 S-Twin microscope working at 200 kV) equipped with X-ray energy-dispersive spectroscopy detector. Thirty microliters of the Bi_2Te_3 colloid were drop-casted on freshly cleaved mica surface. After 10 min adsorption, excessive solutions are withdrawn from the mica surface followed by atomic force electron microscope (AFM) observations. Tapping-mode AFM studies were performed on a Dimension 3100 AFM (Bruker, USA) under ambient conditions. Commercial silicon tips with a nominal spring constant of 2.0 N/m and resonant frequency of 437.2 kHz were used in all the AFM imaging.

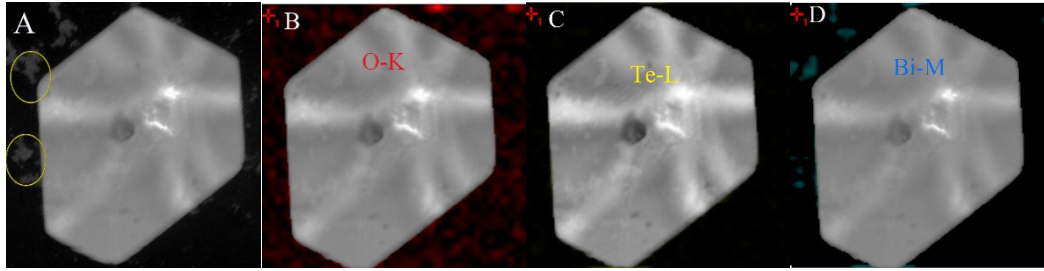


Figure S1. Element mapping of Bi_2O_3 producing during the oxidation of Bi_2Te_3 nanoplates. In order to make clear the composition of nanoparticles besides the Bi_2Te_3 nanoplate, the Bi_2Te_3 nanoplate mapping was deleted: (A) STEM image of Bi_2O_3 nanocrystals (in the yellow line), (B) O mapping; (C) Te mapping which shows that nanocrystals contain none of Te element, confirming the nanocrystal is Bi_2O_3 ; (D) Bi mapping. From B-D, the nanoparticles besides the nanosheet contain O and Bi element without Te element. It indicates that such nanoparticles are Bi_2O_3 which is consistent to the XRD pattern of Bi_2Te_3 after oxidation (Fig. 1 in maintext).

Table S1. Relative intensities comparison of XRD peaks of Bi_2Te_3 nanoplate before and after oxidation by H_2O_2 , comparing to intensity of peak (110).

| Facets | Bulk | Volume of H_2O_2 / mL | | | | |
|----------|------|---------------------------------------|------|------|------|----|
| | | 0 | 0.3 | 0.6 | 0.9 | 3 |
| (0 0 6) | 8 | 6.49 | 7.82 | 16.5 | 25 | 33 |
| (0 0 15) | 6 | 9.15 | 12.3 | 23 | 28.9 | 39 |
| (1 0 10) | 25 | 50.3 | 47 | 50 | 69 | 57 |

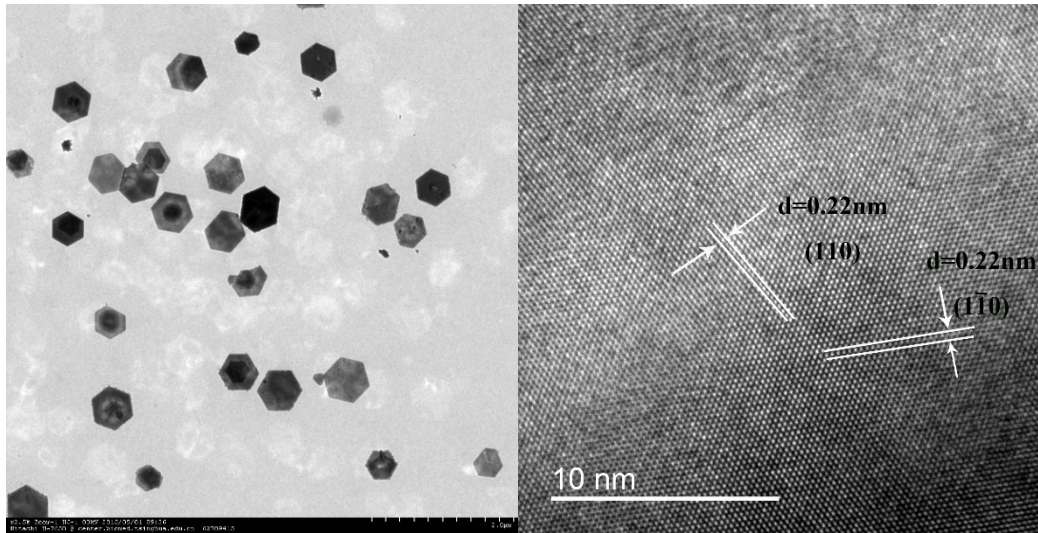


Figure S2. TEM image of Bi_2Te_3 nanoplates with controllable oxidation degree, forming into stair-like nanocrystals (Left); HRTEM image (Right) of thinner part with indexed lattice spacing (0.22 nm) to facets (110) of Bi_2Te_3 .

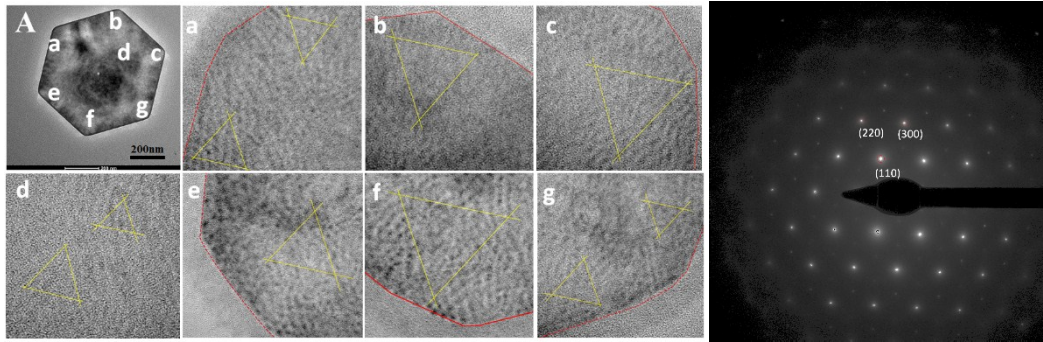


Figure S3. (A) HRTEM images of Bi_2Te_3 nanoplate and its uniform lattice fringes with different department, (B) Electron diffraction of single Bi_2Te_3 nanoplates.

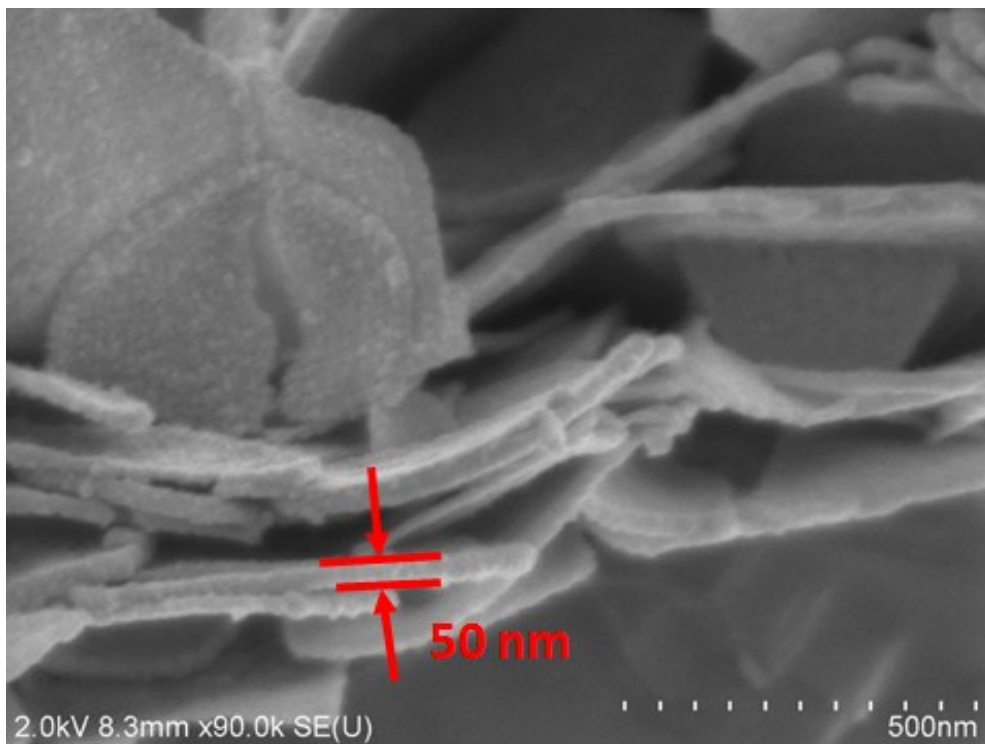


Figure S4. SEM image of as-prepared Bi_2Te_3 nanoplates, which shows the thickness of Bi_2Te_3 nanoplates is about 50 nm.

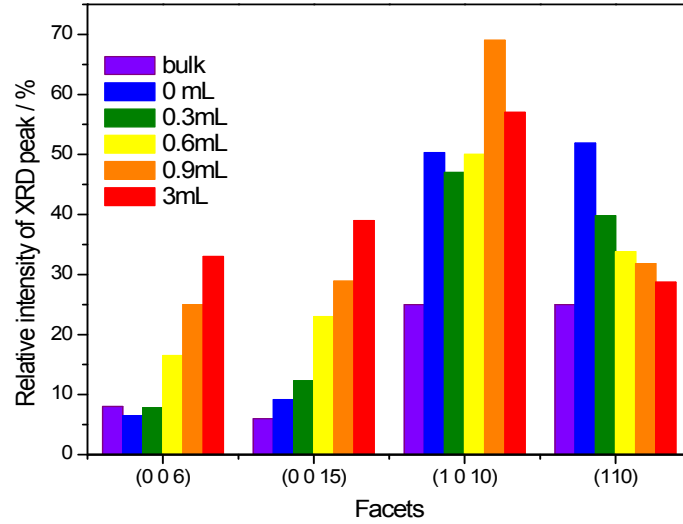


Figure S5. The relative intensities comparison of diffraction peaks (0 0 6), (0 0 15) and (1 0 10), comparing to (015) facets when using different concentrations of H₂O₂. The relative XRD peaks intensities of facets (0 0 6) and (0 0 15) are up to 33% and 39% from 7% and 12.3% in the case of nanoplates.

S-1: Raman spectra characterizations discussion:

In order to further confirm the pure phase of Bi₂Te₃ nanoplate after oxidation, Raman spectra of different individual as-prepared nanoplates were collected (Fig. 4C and S6). The peaks located at 36.8, 61.9, 102 and 135 cm⁻¹ were assigned to the E_g^1 , A_{1g}^1 , E_g^2 , and A_{1g}^2 vibrational modes of Bi₂Te₃ respectively (Table S2)². All of peaks were caused by the vibration of Bi₂Te₃ phase and no any other Raman peaks were observed, which illustrated that no Bi₂O₃ or other oxide phase produced on the Bi₂Te₃ nanoplate during oxidation. The Raman spectra of powder Bi₂Te₃ nanosheets samples after oxidation were also collected. As shown in Figure S7, Raman peaks located at 102 cm⁻¹ and 135 cm⁻¹ should be assigned to E_g^2 , A_{1g}^2 vibrational modes of Bi₂Te₃ nanoplate respectively.² No Raman peaks of any bismuth oxide phase were observed. It also confirmed that no bismuth oxide existed on as-prepared ultrathin Bi₂Te₃ nanosheets.

Table S2. Raman shifts and vibrational modes attribution.

| Raman shift / cm ⁻¹ | Vibrational mode | Raman modes of Bi ₂ Te ₃ ² |
|--------------------------------|------------------|---|
| 36.8 | E_g^1 | |
| 61.9 | A_{1g}^1 | |
| 102 | E_g^2 | |
| 135 | A_{1g}^2 | |

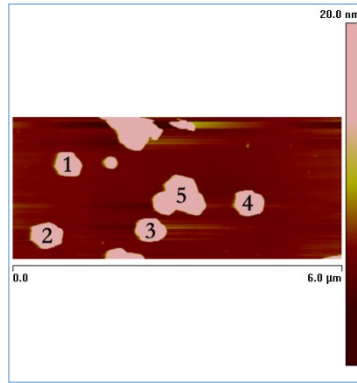


Figure S6. The AFM images of five different individual Bi_2Te_3 nanosheets after chemical corrosion treatment. Then it is labeled for the individual Raman spectra detection.

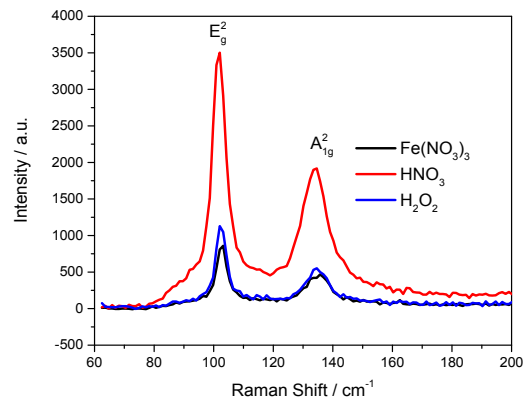


Figure S7. Raman shifts of as-prepared powder Bi_2Te_3 nanosheets sample after oxidation.

Reference:

1. Zhang, Y.; Hu, L. P.; Zhu, T.; Xie, J.; Zhao, X. B. *Cryst. Growth Des.* **2013**, 13, 645.
2. Zhao, Y.; Luo, X.; Zhang, J.; Wu, J.; Bai, X.; Wang, M.; Jia, J.; Peng, H.; Liu, Z.; Quek, S. Y.; Xiong, Q. *Physical Review B* **2014**, 90, 245428.